Calhoun: The NPS Institutional Archive

DSpace Repository

Theses and Dissertations 1. Thesis and Dissertation Collection, all items

1984

Particle sizing from forward scattered light at two angles using a variable-focal-length optical system

Powers, John

http://hdl.handle.net/10945/19491

Downloaded from NPS Archive: Calhoun

Calhoun is the Naval Postgraduate School's public access digital repository for research materials and institutional publications created by the NPS community. Calhoun is named for Professor of Mathematics Guy K. Calhoun, NPS's first appointed -- and published -- scholarly author.

Dudley Knox Library / Naval Postgraduate School
411 Dyer Road / 1 University Circle
Monterey, California USA 93943

http://www.nps.edu/library

DUDLEY KNOX LIBRARY
NAVAL POSTGRADUATE SCHOOL
MONTEREY, CALIFORNIA 93943

NAVAL POSTGRADUATE SCHOOL
Monterey, California

THESIS

PARTICLE SIZING FROM FORWARD SCATTERED LIGHT AT TWO ANGLES USING A VARIABLE-FOCAL-LENGTH OPTICAL SYSTEM

by

John Powers

December 1984

Thesis Advisor: Oscar Biblarz

Approved for public release; distribution unlimited.

T223078

REPORT DOCUMENTATION PAGE

READ INSTRUCTIONS
BEFORE COMPLETING FORM

1. REPORT NUMBER

2. GOVT ACCESSION NO.

3. RECIPIENT'S CATALOG NUMBER

4. TITLE (and Subtitle)
Particle Sizing from Forward Scattered Light
at Two Angles
Using a Variable-Focal-Length Optical System

5. TYPE OF REPORT & PERIOD COVERED
Master's Thesis
December 1984

6. PERFORMING ORG. REPORT NUMBER

7. AUTHOR(s)
John Powers

8. CONTRACT OR GRANT NUMBER(s)

9. PERFORMING ORGANIZATION NAME AND ADDRESS
Naval Postgraduate School
Monterey, California 93943

10. PROGRAM ELEMENT, PROJECT, TASK AREA & WORK UNIT NUMBERS

11. CONTROLLING OFFICE NAME AND ADDRESS
Naval Postgraduate School
Monterey, California 93943

12. REPORT DATE
December 1984

13. NUMBER OF PAGES
47

14. MONITORING AGENCY NAME & ADDRESS(if different from Controlling Office)

15. SECURITY CLASS. (of this report)

15a. DECLASSIFICATION DOWNGRADING SCHEDULE

16. DISTRIBUTION STATEMENT (of this Report)

Approved for public release; distribution unlimited.

17. DISTRIBUTION STATEMENT (of the abstract entered in Block 20, if different from Report)

18. SUPPLEMENTARY NOTES

19. KEY WORDS (Continue on reverse side if necessary and identify by block number)

Particle Measurement, Variable-Focal-Length Optical System

20. ABSTRACT (Continue on reverse side if necessary and identify by block number)

The theory of operation and description of a particle sizing device which indirectly determines the size of small particles from forward scattered light at two angles is presented. The device incorporates a fixed detector geometry and maintains a fixed intensity ratio at two photodiode detectors by adjusting the optical system focal length.

Simple analogue signal processing is used with a servomotor to make continuous adjustments automatically.

The optical device is used to investigate the effects of an applied high intensity electric field on a fuel spray from a turbine engine fuel nozzle for changes in droplet size. Preliminary results on a T-56 nozzle spraying DF-2 fuel at 75 psig with the sample volume 8 centimeters from the nozzle and using a sharp electrode with the point 10 millimeters from the nozzle at a potential of 16 kV showed no conclusive changes in droplet size. The Sauter mean diameter of the fuel spray varied from 42 to 47 microns.

Approved for public release; distribution unlimited.

Particle Sizing from Forward Scattered Light at Two Angles Using a Variable-Focal-Length Optical System

by

John Powers
Lieutenant, United States Navy
B.S., University of San Francisco, 1976

Submitted in partial fulfillment of the
requirements for the degree of

MASTER OF SCIENCE IN AERONAUTICAL ENGINEERING

from the

NAVAL POSTGRADUATE SCHOOL
December 1984

ABSTRACT

The theory of operation and description of a particle sizing device which indirectly determines the size of small particles from forward scattered light at two angles is presented. The device incorporates a fixed detector geometry and maintains a fixed intensity ratio at two photodiode detectors by adjusting the optical system focal length. Simple analogue signal processing is used with a servomotor to make continuous adjustments automatically.

The optical device is used to investigate the effects of an applied high intensity electric field on a fuel spray from a turbine engine fuel nozzle for changes in droplet size. Preliminary results on a T-56 nozzle spraying DF-2 fuel at 75 psig with the sample volume 8 centimeters from the nozzle and using a sharp electrode with the point 10 millimeters from the nozzle at a potential of 16 kV showed no conclusive changes in droplet size. The Sauter mean diameter of the fuel spray varied from 42 to 47 microns.

ACKNOWLEDGEMENTS

To my wife Laurie, with all my love.

TABLE OF CONTENTS

I. INTRODUCTION 9

II. THEORY OF OPERATION 11

    A. SYSTEM OPTICS 15

III. DEVICE DESCRIPTION 27

    A. OPTICS 27

        1. General 27

        2. System Focal Length Calibration 33

    B. ELECTRONICS 34

        1. General 34

        2. Internal Controls and Biasing Procedure 36

        3. External Controls and Connections 38

IV. CONCLUSIONS 41

V. RECOMMENDATIONS 44

LIST OF REFERENCES 45

BIBLIOGRAPHY 46

INITIAL DISTRIBUTION LIST 47

LIST OF TABLES

1. Symbols 10
2. Focal Length vs Micrometer Setting 33
3. Internal Controls (top to bottom) 37

LIST OF FIGURES

2.1 Distribution of Forward-scattered Light (Reproduced from [Ref. 5]) 22
2.2 Relative-intensity Peaks of Fraunhofer Diffraction (Reproduced from [Ref. 5]) 23
2.3 Optical System as Equivalent Thin Lens 24
2.4 Ray Diagram - Confocal Pair 25
2.5 Optical System Ray Diagram (not to scale) 26
3.1 Signal Processing Block Diagram 40
4.1 Typical D_{32} vs Electrode Voltage 42
4.2 Typical Channel Response and Servo Tracking 43

I. INTRODUCTION

The purpose of this thesis is to describe the conception, design, and initial development of a particle sizing device employing a variable-focal-length optical system.

This work was undertaken to facilitate ongoing studies at the Naval Postgraduate School investigating the effects of high-intensity electric fields on the spray from a gas turbine engine fuel nozzle. These effects include a demonstrated improvement in combustion efficiency [Ref. 1]. Previous work under room temperature conditions by Laib [Ref. 2] has shown that the spray angle from the nozzle is increased and that the intensity of light from a laser beam transiting the spray pattern could be decreased by a small percentage by the application of a strong electric field. More precise measurements under ambient conditions by Zajdman [Ref. 3] has shown that the transmitted light from a laser could be decreased by as much as two percent.

It has been theorized that these effects on the fuel spray caused by the application of high intensity electric fields could be explained by a resultant decrease in the average particle size.

The purpose of this thesis is to develop a device which allows the determination of the Sauter mean diameter (D_{32}) of the fuel spray from the intensity of forward scattered light at two angles in an effort to detect a change in droplet size directly.

Investigation of droplet size measuring techniques by this method suggested an innovation in methodology using a zoom lens in the optical system. The result of the innovation allows measurements to be taken with fixed detector geometry and optimum signal ratio for Sauter mean diameter determination over a three-to-one size ratio. Multiple diode pairs increase the Sauter mean diameter range to the aperture limits of the device. Simple analogue signal processing has been incorporated which allows a servo system to make continuous adjustments of the focal length for changes in Sauter mean diameter automatically.

TABLE 1
Symbols

Symbol	Definition
α	particle size parameter
$\alpha\theta$	beam spread parameter
D	Sauter mean diameter
f	focal length
I	intensity
J	first-order Bessel function
λ	wavelength
n	multiple of objective focal lengths
r	aperture radius
s_o	object distance
s_i	image distance
θ	angle between ray and optical centerline
x	off-center distance at detector plane

II. THEORY OF OPERATION

A complete explanation of light scattering by small particles was written by H.C. Van de Hulst [Ref. 4]. A very useful paper on the measurement of particle size from forward scattered light was written by Donald R. Buchele [Ref. 5]. from which Figure 2.1 is reproduced, along with the following explanation. Useful approximations for the intensity distribution of forward-scattered light in the center lobe are plotted in Figure 2.1 The ordinate is the intensity at a scattering angle θ divided by the intensity at $\theta = 0$, the direction of the incident light. The abscissa is the square of the dimensionless beam spread parameter where the particle size parameter is

$$\alpha = \pi D/\lambda \tag{2.1}$$

with particle diameter D and wavelength λ.

The curve for a monodispersion is given by Fraunhofer diffraction [Ref. 6], where J_1 is the first-order Bessel function. For $\theta < 20^0$, $\sin\theta$ may be replaced by θ in radians.

$$I(\theta)/I(0) = [2J_1(\theta\sin\theta)/(\theta\sin\theta)]^2 \tag{2.2}$$

The two curves for a polydispersion of particles are based on the Sauter mean diameter D_{32}. This diameter is the ratio of total particle volume to total particle surface area. The curves were derived in [Ref. 7] and [Ref. 8] using the monodisperse function with a wide variety of particle- diameter distributions in which no particles exist with a diameter larger than approximately ten times the Sauter mean diameter.

The Gaussian curve is a good approximation to the other curves, and it is a good approximation to the curve found in [Ref. 9], best representing the intensity distribution of light scattered by fuel spray. At $\alpha\theta < 3$, all curves in Figure 2.1 agree with each other within 5 percent of full scale [Ref. 5].

The Gaussian approximation of scattering gives the ratio of intensities at two angles as

$$I_2/I_1 = \exp(0.57)^2[(\alpha\theta_1)^2 - (\alpha\theta_2)^2] \qquad (2.3)$$

or

$$I_1/I_0 = \exp[-(0.57)^2(\alpha\theta_1)^2] \qquad (2.4)$$

Let x_1 and x_2 be the distances at the detector plane corresponding to θ_1 and θ_2 for a given focal length. Using the small angle approximation,

$$\theta = x/f \qquad (2.5)$$

Let x_1 and x_2 be constant by design. For some range of particle sizes, let I_2/I_1 be kept constant by varying f with D_{32}. Using Equation 2.5 to substitute for θ_1 and θ_2 in Equation 2.3 and using Equation 2.1 to substitute for α and rearranging,

$$(D_{32}/f)^2 = \ln(I_2/I_1)(\lambda/0.57\pi)^2/(x_1^2 - x_2^2) \qquad (2.6)$$

Thus by method and design, D_{32}/f can be held constant. If D_{32}/f is held constant, then Equation 2.7 shows that the beam spread parameters $\alpha\theta_1$ and $\alpha\theta_2$ are also held constant for constant x_1 and x_2. Equation 2.7 is derived by equating the product of both sides of Equation 2.1 and Equation 2.5 .

$$\alpha\theta = x(\pi/\lambda)(D_{32}/f) \qquad (2.7)$$

One can measure x_1, x_2, and f directly. In order both to solve Equation 2.6 for D_{32} and to validate the assumptions, I_2/I_1 must be known and held constant, respectively. One should choose $\alpha\theta_1$ and $\alpha\theta_2$ to maximize changes in I_2/I_1 with percent changes in D_{32}. In other words, one should maximize $d(I_2/I_1)/(dD_{32}/D_{32})$ with respect to $\alpha\theta_1$ and $\alpha\theta_2$.

Differentiating Equation 2.3 and rearranging yields Equation 2.8.

$$d(I_2/I_1)/(dD_{32}/D_{32}) = 2(0.57)^2[(\alpha\theta_1)^2 - (\alpha\theta_2)^2] \\ *\exp(0.57)^2[(\alpha\theta_1)^2 - (\alpha\theta_2)^2] \qquad (2.8)$$

Differentiating Equation 2.8 with respect to $\alpha\theta_2$, setting equal to zero, and simplifying yields Equation 2.9.

$$(\alpha\theta_2)^2 = (\alpha\theta_1)^2 + 1/(0.57)^2 \qquad (2.9)$$

Differentiating Equation 2.8 with respect to $\alpha\theta_1$, setting equal to zero and simplifying yields the same result.

Granting this condition leaves one remaining degree of freedom. Let $\alpha\theta_1$ be chosen such that $d(I_1/I_0)/(dD_{32}/D_{32})$ is maximized for a given D_{32}. Differentiating Equation 2.4 and rearranging yields Equation 2.10.

$$d(I_1/I_0)/(dD_{32}/D_{32}) = -2(0.57)^2(\alpha\theta_1)^2 \\ *\exp[-(0.57)^2(\alpha\theta_1)^2] \qquad (2.10)$$

Setting the partial derivative of Equation 2.10 with respect to $\alpha\theta_1$ equal to zero yields Equation 2.11.

$$\alpha\theta_1 = 1/0.57 \qquad (2.11)$$

Solving Equations 2.9 and 2.11 for $\alpha\theta_2$ yields Equation 2.12 .

$$\alpha\theta_2 = \sqrt{2}/0.57 \qquad (2.12)$$

Equations 2.11 and 2.12 together yield the required detector geometry ratio given by Equation 2.13 .

$$x_2/x_1 = \alpha\theta_2/\alpha\theta_1 = \sqrt{2} \qquad (2.13)$$

Substituting the expressions for $\alpha\theta_1$ and $\alpha\theta_2$ from Equations 2.11 and 2.12 into Equation 2.3 yields the required signal ratio given by Equation 2.14 .

$$I_2/I_1 = 1/e \qquad (2.14)$$

Substitution of the same results into Equation 2.8 yields Equation 2.15 .

$$d(I_2/I_1)/(dD_{32}/D_{32}) = -2/e \qquad (2.15)$$

A similar substitution into Equation 2.10 yields Equation 2.16 .

$$d(I_1/I_0)/(dD_{32}/D_{32}) = -2/e \qquad (2.16)$$

Finally, substitution of $x_2 = \sqrt{2}x_1$ and $I_2/I_1 = 1/e$ into Equation 2.6 and solving for D_{32} yields Equation 2.17 .

$$D_{32} = f(\lambda/0.57\pi x_1) \qquad (2.17)$$

Figure 2.2 from [Ref. 5] shows a relative intensity $I(\theta,D)/I(0,D)$ for a circular particle as a function of angle θ and diameter D (D = 10,000 microns, λ = 1 micron.) For clarity, the intensity at θ and D have been arbitrarily divided by the intensity at $\theta = 0$ and $D = 0$. From the figure, one can see that for a given number of scattering particles, the relative intensity is directly proportional to the fourth power of D_{32} at constant focal length. Since the intensity in an optical system is inversely proportional to the square of the focal length, and Equation 2.17 shows a linear relationship holds between f and D_{32} for the measuring method described, we conclude that for the method described, relative intensity will be directly proportional to the square of D_{32} for a constant number of effective scattering particles.

A. SYSTEM OPTICS

The angles involved for measuring particle sizes of 50 to 300 microns by the method described are between 1.178 milliradians for θ_1 at 300 microns and 9.995 milliradians for θ_2 at 50 microns. Therefore, the small angle approximations and the principles of first-order optics are excellent if highly corrected, high quality commercial lenses are used.

The optical principles used to design this system are fully explained in any good basic optics text, such as [Ref. 10], and are as follows:

1. Light incident to the forward principal plane at the optic axis leaves the lens element at the aft principal plane at the optic axis travelling in the same direction in space.

2. Parallel rays incident to the lens forward principal plane arrive at the same point on the plane perpendicular to the optic axis at the aft focal point.

The following useful corollary to the first two principles is obtained by applying the first principle to a ray coincident with the optic axis and applying the second principle to all parallel rays to this first ray.

3. All incident rays parallel to the optic axis pass through the aft focal point.

Another useful, easily proved corollary is

4. All rays which pass through the forward focal point emerge from the lens parallel to the optic axis.

A useful equation for aligning and focusing the system is the Gaussian Lens Equation. This equation states that the reciprocal of the focal length is equal to the sum of the reciprocals of the object and image distances. These are the signed distances from the forward principal plane to the object and from the aft principal plane to the image, respectively.

$$1/f = 1/s_o + 1/s_i \qquad (2.18)$$

Figure 2.3 shows two thin lens diagram equivalents for the overall optical system, one with the focal length double that of the other. The optical system must bring the unscattered light to a point on the detector plane that does not move with changes in focal length. This can be accomplished by keeping the aft focal point on the detector plane and orienting the optic axis to be parallel to the unscattered light source direction. Aperture requirements will be minimized by making the light source ray and the optic axis coincident. A measure of the success of meeting this requirement and for verifying that the final design is free of distortions is the image quality when using a viewing screen at the detector plane for an image coming into the optical system from infinite distance, such as the image of a reticle in a precision collimator.

The easiest way to meet these conditions with changing focal length is to properly incorporate a zoom lens as a lens element into the system.

An ideal zoom lens keeps the image position constant while zooming, or varying the focal length of the lens with the focus set for a given object distance. High quality commercial zoom lenses are readily available for use with cameras. The desired image position for the camera is on the film plane. From this basic property and the lens equation, it follows that when the zoom lens is set at infinite object distance, the aft focal point is located at the film plane, and does not move when zooming the lens. Therefore, the key to incorporating the zoom lens in this application is to set the focus for infinite object distance. To incorporate the zoom lens in the forward direction (pointing toward the fuel spray) as an element in the optical system, have it follow an element with infinite image distance for an image originally from infinite distance to the system, and have the desired image point for the next element at what would be the film plane if the zoom lens were mounted on a camera. To incorporate the zoom lens pointing aft, have it follow an element with the image point for the element preceding the zoom lens at the film plane, and the desired object distance for the next element be at infinity.

From the element following the zoom lens, the image must then ultimately be put on the detector plane in such a way that the desired focal length range is obtained without exceeding any of the aperture requirements of the lenses one has available for elements.

The optical system used in this work has the zoom lens pointing in the forward direction, and unless specifically stated otherwise, the following analysis assumes this condition.

Since the zoom lens would focus the collimator image on the focal plane all by itself, the zoom lens could have been used alone as the entire optical system. This system would have some unacceptable disadvantages. A great deal of scattering of the transmitted beam would be caused by the zoom lens itself. It is highly desireable to be able to block the transmitted beam and all angles not of interest just after a low-scattering first lens element.

The focal lengths of reasonably priced high quality zoom lenses are relatively small. The optical system used for this thesis has a useable focal length range of 1959.2 mm to 5104.6 mm, which allows the use of quiet, highly sensitive, large active area, discrete photodiodes, which cannot be placed any closer than about 10 mm apart. Each channel can be individually zeroed for the light not actually scattered by the particles, and provides a continuous analog signal.

Figure 2.4 shows a pair of lens elements placed so that the aft focal point of the first lens element is coincident with the forward focal point of the aft element. Successive application of Equation 2.18 shows that for this combination, an infinite object distance results in an infinite image distance. The image distance for a lens element following this combination under these conditions would be equal to its focal length regardless of its position, so engineering convenience could be used as a criterion for its placement, with due regard for its aperture requirements and those of the downstream elements. The superimposed ray diagram on the confocal pair in Figure 2.4 shows that the incident and emergent angles of a pencil of light with the optic axis, θ_i and θ_e, and the fore and aft element focal lengths are related by Equation 2.19 .

$$\theta_e / \theta_i = f_f / f_a \qquad (2.19)$$

Successive application of Equation 2.19 for a series of i confocal pairs shows that the relation between the incident and emergent angles is governed by Equation 2.20 .

$$\theta_e/\theta_i = \prod_i (f_f/f_a)_i \qquad (2.20)$$

Rearrangement of Equation 2.5 shows that for any single lens element, or for the optical system as a whole (itself useable as a combined lens element), Equation 2.21 applies.

$$f = x/\theta_i \qquad (2.21)$$

The optical system used for this work uses two confocal lens element pairs followed by a single lens element with the aft-focal point on the detector plane. The first element of the second confocal pair is a zoom lens.

Applying Equation 2.21 to the system as a whole yields Equation 2.22 .

$$f_{sys} = x/\theta_i \qquad (2.22)$$

Applying Equation 2.21 to the last lens element, and noting that the incident angle for the last lens element is the emergent angle for the confocal pair series, yields Equation 2.23 .

$$f_5 = x/\theta_e \qquad (2.23)$$

Substituting Equation 2.23 into Equation 2.22 yields Equation 2.24 .

$$f_{sys} = (\theta_e/\theta_i)\, f_5 \qquad (2.24)$$

Substituting Equation 2.20 into Equation 2.24 yields the desired focal length expression for the optical system in terms of the focal lengths of the individual elements (Equation 2.25).

$$f_{sys} = (f_1/f_2)(f_3/f_4)f_5 \qquad (2.25)$$

Figure 2.5 is an equivalent thin lens ray diagram for Figure 2.3 in terms of the individual lens elements of the optical system, not to actual scale, which illustrates the validity of Equation 2.25 .

The planes containing the confocal points are special in that diffraction effects of pinholes, stops, and slits have no effect on image quality at the detector plane because the arrival point of a ray of light at the detector plane is dependent only on the position the light came from the confocal plane, not on its direction. In optics textbooks, these planes are referred to as transform planes for the aggregate elements which consist of the elements in front of the planes [Ref. 11].

Therefore, a slit of just sufficient length and width to illuminate the detector pinhole apertures at all zoom settings is located at the confocal plane of the first confocal pair. The pinhole apertures themselves are located on a removeable diaphragm at the confocal plane of the second confocal pair, which corresponds to the film plane for the zoom lens. Examination of Figure 2.5 for a ray constructed using the basic principles of optics and basic geometry which crosses the optic axis n-objective focal lengths in front of the forward objective principal plane, provides the following recursive relations from the aperture radii at the principal plane for each of the lens elements in millimeters, where c_1 is the distance in millimeters between the aft-focal point of the zoom lens and the aft principal plane of the second lens element, and c_2 is the distance between the aft principle plane of the fourth lens element and the forward principle plane of the last lens element.

$$r_1 = \tan(\theta)(n)f_1 \qquad (2.26)$$

$$r_2 = \tan(\theta)[f_1 + (1 - n)f_2] \qquad (2.27)$$

$$r_3 = r_2 - [(c_1 - f_3)\tan(\theta)(f_1)/f_2] \qquad (2.28)$$

$$r_4 = r_i + [(r_i - r_3)(f_4)/f_3] \qquad (2.29)$$

$$r_5 = r_4 - (r_i)(c_2)/f_5 \qquad (2.30)$$

Equation 2.31 relates the angle θ that a ray makes with the axis of the optical system to the zoom lens focal length for a given off-axis pinhole location r_i when the pinhole aperture is located at the zoom lens aft focal plane.

$$r_i = -\tan(\theta)(f_1)(f_3)/f_2 \qquad (2.31)$$

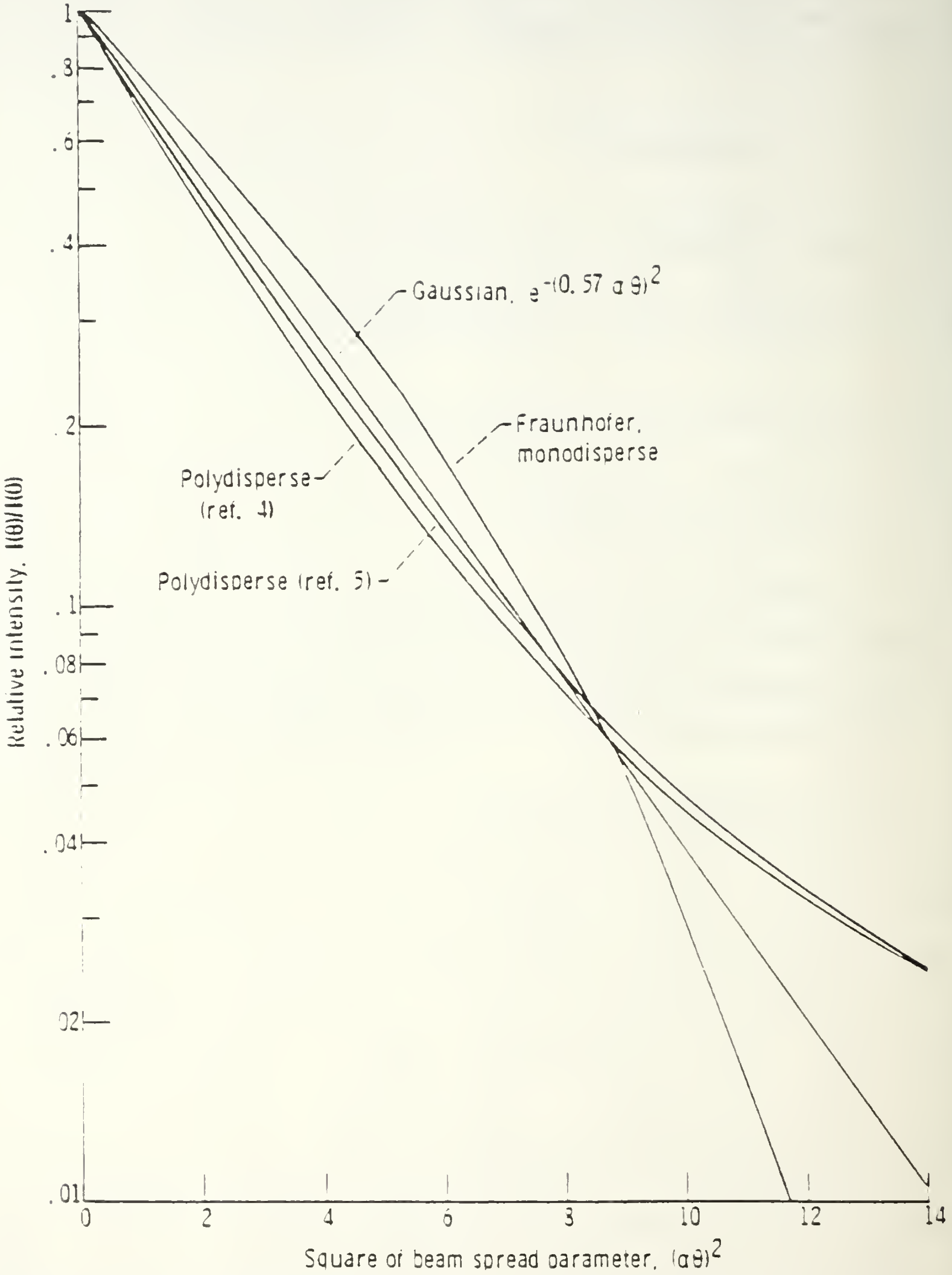

Figure 2.1 Distribution of Forward-scattered Light (Reproduced from [Ref. 5]).

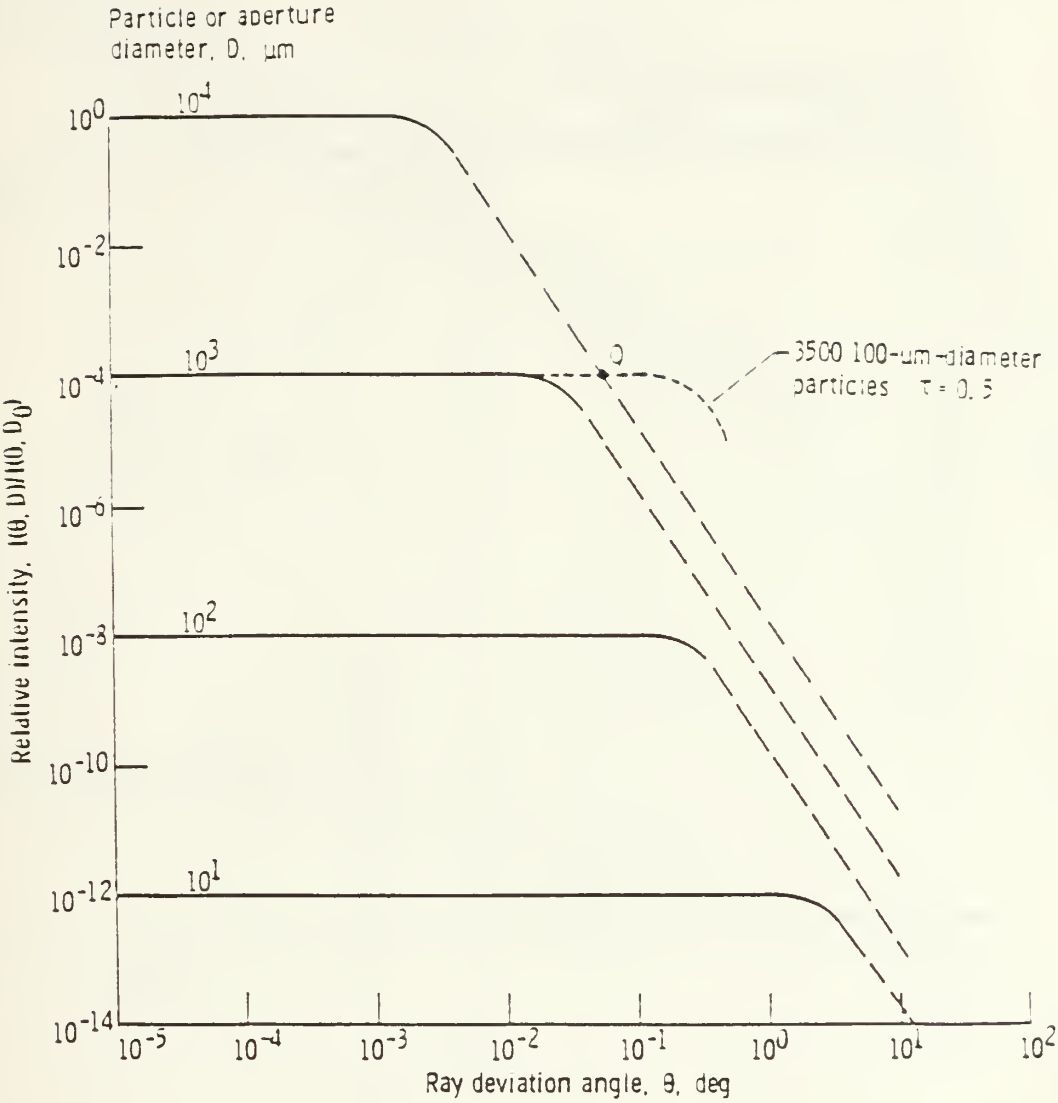

Figure 2.2 Relative-intensity Peaks of Fraunhofer Diffraction (Reproduced from [Ref. 5]).

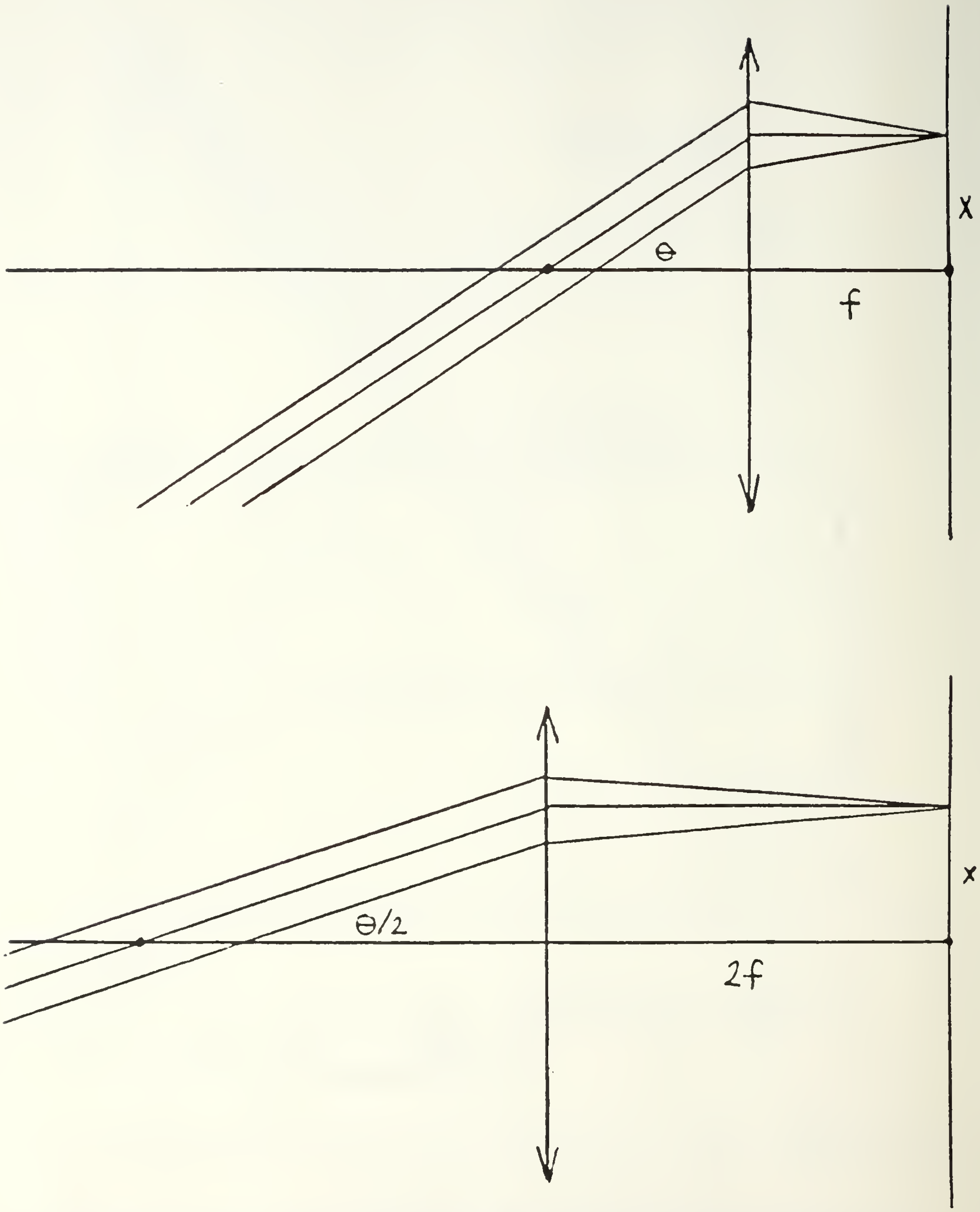

Figure 2.3 Optical System as Equivalent Thin Lens

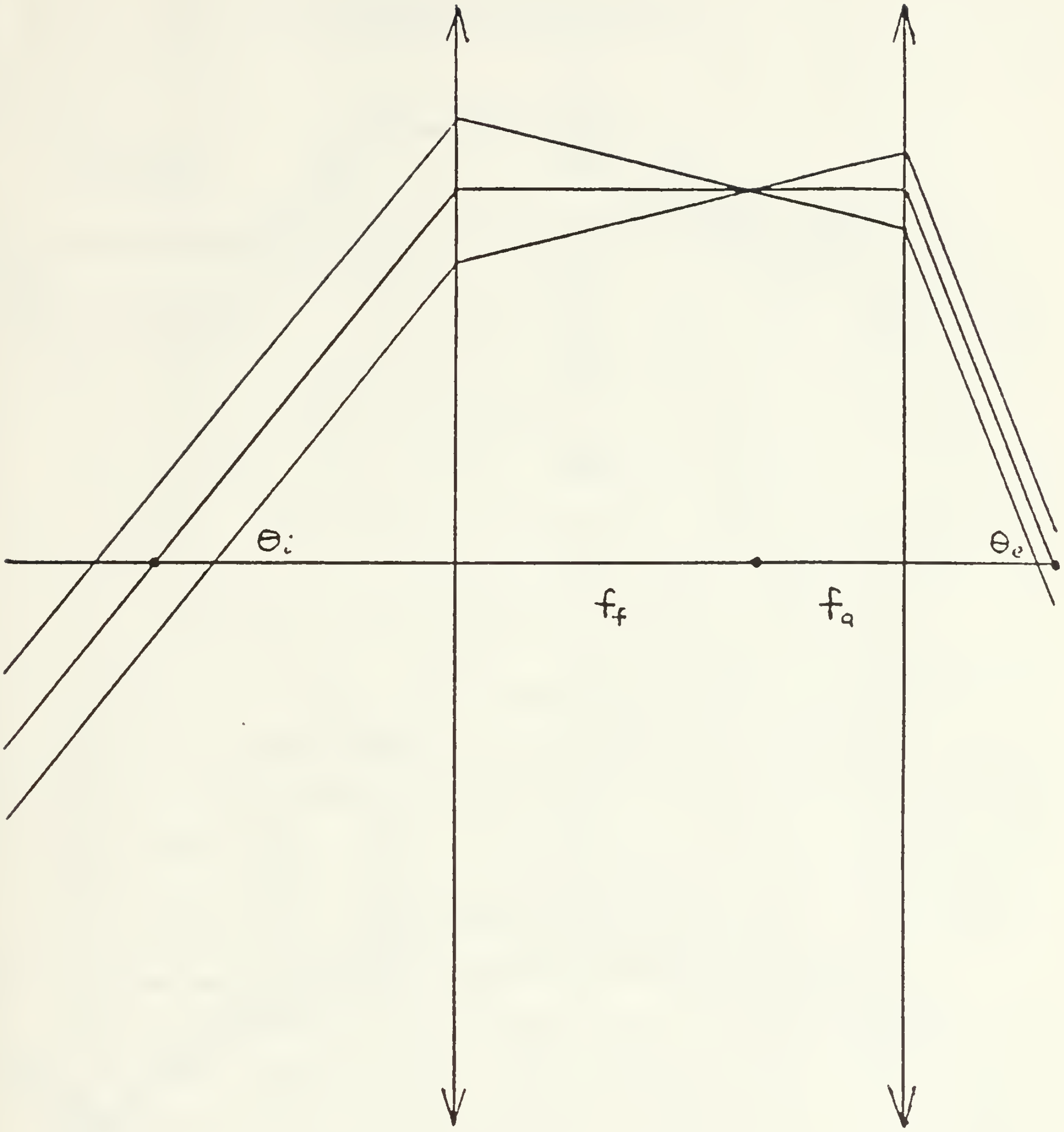

Figure 2.4   Ray Diagram - Confocal Pair

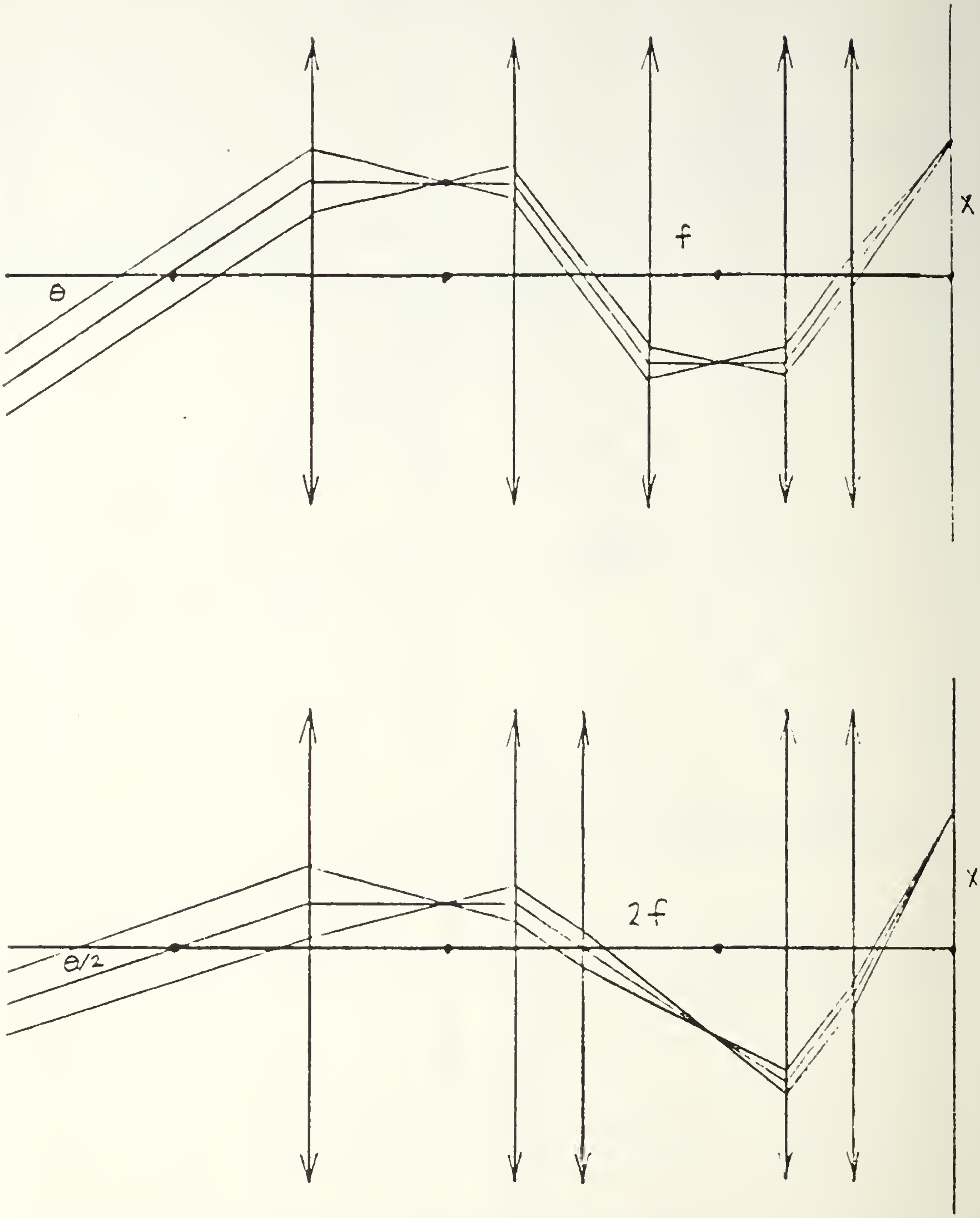

Figure 2.5 Optical System Ray Diagram (not to scale)

III. DEVICE DESCRIPTION

A. OPTICS

1. General

The optical system consists of five lens elements aligned in series as shown in Figure 2.5 . The first lens element consists of an objective lens for an opaque projector, with a nominal focal length of 26 inches (660 mm) and a nominal aperture diameter of 4 inches (f/number = 6.5). The second and fifth elements consist of high quality, highly corrected, wide-angle aspherical lenses originally designed for use in aerial photography cameras. They have a nominal focal length of six inches and an f/number equal to 6.5. Their exact backward and forward focal lengths as measured from the lens surfaces are provided by the manufacturer to the nearest thousandth of an inch. The third lens element is a nominal 70 to 210 mm Series-One zoom lens made by Vivitar, with an f/number of 3.5. The fourth lens element is a nominal 25 mm lens originally designed for use on a closed-circuit television camera. It has an f/number of 1.4.

The lens elements and detector platform pedestal are mounted on the central axis cf four parallel 0.500-inch thick aluminum plates, 9.875 inches in diameter. Each pair of plates is held rigidly parallel by three half inch diameter steel rods 120 degrees apart 0.625 inches from the the plate edges. The rods are staggered 60 degrees from section to section to allow for fasteners.

The objective is mounted on the first plate in a sleeve with a set screw, and the poles between the first and second plate are machined so that the objective can slide fore and aft about 0.5 inch from the position where its aft focal point rests on the front surface of a stage which is mounted on the second lens element so that this surface contains the forward focal plane of the second lens element. This stage has a 1.0 inch diameter hole in the center over which a slit aperture is glued after the system has been focused and calibrated for focal length versus micrometric screw setting. In the center of the slit is a small stop whose total width (1.0 mm) subtends 1.5 milliradians at the nominal objective focal length. A 400 micron clearance aperture is in the center of the stop which is unobstructed when aligning the central beam, and can be blocked by putting tension on a string painted flat black. This arrangement dramatically decreases the scattering of the main beam by the lens elements and does not interfere with the signal at any angle of interest.

The second lens element is mounted on the front of the second plate. On the reverse side of the second plate the zoom drive mechanism is mounted. The zoom drive mechanism consists of a sleeve mounted on the zoom lens adjust barrel which is driven fore and aft for zooming action by a precision-made micrometric screw. The micrometeric screw advances one tenth of an inch for every four revolutions of the micrometric screw. The screw is graduated to the nearest thousandth of an inch. Approximately thirty millimeters of travel are required to traverse the full zoom range. Approximately one half turn of the micrometric screw is avoided on each end of the zoom range to preclude disturbing the calibration of system focal length versus micrometric screw setting. The micrometric screw is geared to a 15 turn potentiometer by a 22 to 96 teeth gear ratio. The potentiometer is used as a variable resistance to a constant voltage which is used as a summing input to an operational amplifier. The potentiometer is in turn geared to a 28 volt DC motor by a 22 to 96 teeth gear ratio. This motor is a high torque, low speed motor, and full traversal of the zoom range at maximum applied voltage of 28 volts requires about 20 seconds. Approximately one turn of the potentiometer on each end of the 15 turn potentiometer is not used.

The zoom drive system was originally designed with an interlocking cogged wheel arrangement located on the micrometric drive axle which allowed for the actuation of microswitches which interrupted drive power when the limits of zoom travel were reached. This mechanism was discarded when it was determined that the mechanism was allowing the zoom adjust barrel to wobble slightly when being changed. This wobbling action could only be detected by observing the image from a precision collimator at the detector plane under a binocular microscope with a magnification of 40X.

The zoom lens is mounted on a tube which is counterbored internally for a diaphragm. The depth of the counterbore is such that the rear surface of the 0.02 inch thick diaphragm is at the film plane distance from the zoom lens mounting plane as specified by the zoom lens manufacturer. The outer surface of the tube is threaded and is screwed into an internally threaded tube along with two lock-rings. The outer tube is threaded on the aft end to to mount on the front face of the third mounting plate. Since the both the zoom lens and the zoom adjust assembly are both rigidly mounted to the system frame, the tolerances for positioning of the zooming elements of the zoom lens assured by the drive system can be better than those assured by the manufacture of the lens with respect to parallelism of the elements, as was done when the wobble with zooming action was eliminated.

The center of the diaphragm has a one half inch diameter hole in the center. A piece of 0.002 inch thick aluminum shim stock with pinhole apertures is glued onto the aft surface of the diaphragm. All the pinhole apertures are within the image of the aperture slit located at the aft focal point of the objective. There is a 50 micron diameter pinhole in the center which is located precisely on the optic axis of the zoom lens. This hole is used when verifying the alignment of the system. In addition, there is a clearance aperture pinhole at this plane for each photodetector at the detector plane. The image formed at the detector plane is slightly oversized, so that the effective aperture is the active area of the photodiode itself.

The fourth lens element is threaded to mount in a 0.125 inch thick plate which is mounted by screws onto the reverse side of the third mounting plate. The length of the tube on which the zoom lens is mounted is adjusted so that the front focal length of the fourth lens element lies on the aft surface of the diaphragm, coincident with the aft focal point of the zoom lens. The last lens element is mounted over the 0.125 inch thick plate on the reverse side of the third mounting plate.

A removable platform is mounted onto the last lens element such that the front face of the platform is coincident with its aft focal plane. This platform is made of plexiglass and the surface facing the spray has been sandblasted to serve as a medium-resolution viewing screen for real images formed by the optical system.

The photodiode detectors are HAD-1100 integral photodiode-op amp combinations manufactured by EG&G. Only the photodiode part of the package is used in this application. Each photodiode is individually mounted in an assembly which has posts on which the electrical leads may be fastened. The photodiode assemblies are mounted on a 0.125 inch thick plate which is in turn mounted on an x-y positioning stage. This stage is mounted on a pedestal which slides in a hole in the center of the last mounting plate. This allows the x-y positioning stage to be rotated or to be moved fore and aft so that the photosensitive surfaces of the photodiodes may be placed at the aft focal plane of the last lens element. Two pairs of photodiodes are installed so that two ranges of particle sizes are available by the turn of a switch. For the inner pair of diodes, the off-center locations of the diodes are 5.71 mm and 8.08 mm, and the outer pair are located at 15.71 and 22.22 mm. The ratio of off-enter distances for both pairs of photodiodes is equal to the square root of two. Switching is available for ten photodiode pairs.

Electrical circuitry providing the two channel outputs and the initial servo signal is on a circuit board mounted on the last mounting plate, along with the diode pair selection switch. The spaces between the first two and last two mounting plates are covered and metal-lined to shield the instrument from extraneous light and electrical noise. Sight holes are placed in the covers so that the 400 micron aperture at the aft objective focal point is visible from behind, and the point where the unobstructed transmitted beam impinges on the detector plane is visible. Alignment is assured when a bright spot can be seen on the detector plane, then tension is placed on the string which blocks the 400 micron aperture, and the sight holes are then covered with opaque tape. The optical path between the second and third mounting plates is enclosed by the zoom adjust assembly and the zoom lens with its mounting tube. The first three mounting planes are threaded for posts on the base which are placed in mounting brackets, and the whole device is mounted on an optical bench.

The scattering volume of fuel spray was approximated by a cylinder of the diameter of a 5 milliwatt Helium-Neon laser manufactured by Hughes, expanded and spatially filtered to a beam diameter of 8.4 mm at a nominal distance of 3 objective focal lengths from the objective. The wavelength of the laser output is 0.6238 microns. Extending the rays from all possible locations within the scattering volume to the optic axis gives an equivalent range of points of origin from the optic axis which can be spanned to determine the maximum aperture requirement for each lens element for a give angle of incidence. All the aperture requirements are exceeded by the lens elements.

The initial focusing and calibration of the optical system is greatly facilitated by the use of a precision collimator. The collimator used for this work was designed for use as an optical strain gauge, and was calibrated by the National Bureau of Standards.

The first step in focusing the system is to project the image of the reticle in the collimator into the objective, and slide the objective in its sleeve until the image of the reticle is in focus on the stage mounted on the second lens element.

The second step in focusing the optical system is best accomplished when the pinhole apertures are not yet glued into place on the diaphragm at the aft zoom focal point. In place of the pinhole apertures is placed a reticle on a piece of glass with the markings on the face towards the objective. The zoom mounting tube is then adjusted so that the image of the reticle is focused on the detector plane screen, and the locking rings are then tightened. When the optical system is assembled with the zoom lens focus adjust set for infinite object distance, the image from the precision collimator is in focus at the detector plane to the aperture limits and maintains focus throughout the zoom range.

2. System Focal Length Calibration

The optical system is calibrated by attaching the reticle used for focusing the device to the detector plane viewing screen on the optical centerline, and superimposing the image of the reticle from the collimator. The reticle at the detector plane is 18 mm long and is graduated in tenths of a millimeter. Since it was originally designed for use with a deflected reflector, the image from the collimator is nominally calibrated in double milliradians with a correction factor supplied by the National Bureau of Standards. Hence, the focal length of the system at a given zoom micrometer setting can be determined by measuring the distance between graduations of the collimator image with the detector plane reticle. This can be done with the help of a 40x- binocular microscope, and the results of this operation are presented in Table 2 .

TABLE 2

Focal Length vs Micrometer Setting

m(in)	f(mm)	m(in)	f(mm)
1.375	1959.2	0.800	2909.8
1.350	1987.2	0.775	2979.1
1.325	2016.9	0.750	3046.7
1.300	2043.0	0.725	3119.6
1.275	2071.4	0.700	3183.4
1.250	2103.4	0.675	3258.1
1.225	2133.9	0.650	3340.8
1.200	2171.5	0.625	3440.4
1.175	2206.9	0.600	3529.6
1.150	2242.3	0.575	3615.1
1.125	2280.3	0.550	3732.8
1.100	2319.6	0.525	3814.7
1.075	2360.0	0.500	3941.7
1.050	2406.5	0.475	4058.7
1.025	2446.1	0.450	4180.8
1.000	2488.5	0.425	4282.8
0.975	2536.9	0.400	4415.7
0.950	2583.7	0.375	4523.6
0.925	2634.7	0.350	4625.9
0.900	2686.1	0.325	4739.4
0.875	2739.0	0.300	4833.8
0.850	2792.1	0.275	4970.7
0.825	2850.2	0.250	5104.6

B. ELECTRONICS

1. General

A simplified block diagram of the signal processing is provided in Figure 3.1

The photodiodes are positioned in pairs so that they produce voltage signals proportional to I_1 and I_2 from Equation 2.3, henceforth referred to as channel 1 and channel 2. A pair of photodiodes are selected by the photodiode pair selector switch. This switch is a multiple wafer rotary switch with one wafer which selects the signal lead for channel 1 and another wafer for channel 2 . The photodiodes are all grounded and provision has been made for applying up to 90 volts of bias to operate the photodiodes photoconductively if desired. It is felt that for sensitivity and linearity of response that the photodiodes are best operated in the photovoltaic mode by grounding the bias leads.

Each channel is connected to the inverting input pin of a LM741- operational amplifier. A gain ratio of 1/e is maintained between channels 1 and 2 by adjusting a variable gain resistance of 100 to 200 kilohms for channel 2 and 33 to 133 kilohms for channel 1. After this point, the two channel outputs are equal at the zero error condition. Therefore, any deviation of the amplification from linear amplification will not in itself cause an error in the ultimate servo signal as long as each channel is identical from this point to where the servo signal is generated.

Each channel is then fed into the inverting input of a LM741- operational amplifier with an overall gain of 20 for the application in this work. The zeroing control for the overall channel output is the offset potentiometer for this operational amplifier. The output from this operational amplifier is then fed into the inverting input of another LM741-operational amplifier with an overall gain of 20, followed by a another operational amplifier which is configured as a non-inverting, voltage-controlled voltage source, second-order, unity gain low-pass filter with a time constant of 0.1 seconds.

The two channel outputs are then connected to two separate pens on a strip chart recorder. In addition, the two outputs are connected to a network made from a standard application of a LM324 quad operational amp lifier and a RA201 precision resistor chip which produces a single output which is proportional to the difference of the input signals. The proportionality constant (gain) can be set from 1 to 995 by following the directions for pin interconnection supplied by the resistance chip manufacturer. A gain of 199 is used in this application. The zero position of the single ended output is controlled by using the third amplifier in the LM324 chip as a summing amplifier for the generated signal and for a potential governed by an external potentiometer.

This output is connected to a low pass filter identical to those previously described, and that output is connected to the third pen of the three pen strip chart recorder and to the inverting input of the preamplifier of a Hyband DC Servo Amplifier Model 150A, which currently has a gain of 10. The DC motor is connected to the servoamplifier such that a positive error signal drives the zoom motor in the direction of increasing focal length. This drives the error signal to zero and maintains an intensity ratio of 1/e for the photodiode pair.

An additional two pen strip chart is necessary to record a signal which is a function of zoom micrometer position, and a voltage which is proportional to the applied voltage on the electrode in the fuel spray pattern. The 10 kilohm potentiometer geared to the zoom micrometer is used in a single-ended fashion and is connected in series with a resistor which is connected to a Zener diode controlled potential of -10.62 Volts. The other end of the potentiometer is connected to the inverting input of a LM741-operational amplifier which is used as a summing amplifier. A 100 kilohm potentiometer is connected in similar fashion in series with a resistor which is connected to a Zener diode controlled potential of +10.62 Volts, with the other end of the potentiometer connected to the inverting input of the summing amplifier. This potentiometer is used to zero the output of the summing amplifier at any arbitrary zoom micrometer setting. Chart control gain may be used to get a wide range of desired sensitivity of pen deflection vs micrometer position.

2. Internal Controls and Biasing Procedure

The main circuitry card has 10 potentiometers in the upper right hand corner which are listed as they appear on the card from top to bottom with a description of their function in Table 3 . Regular adjustment of these controls is not required, but is recommended in the event that any of the electrical components on the card have to be replaced.

The gain resistors may be set by measuring the resistance over the input and output pins of the first stage amplifier of the channel of interest. The actual channel gain ratio may be calculated and fine-adjusted by using a small laser with a variable-reflectivity beam splitter to control the transmitted intensity and a precision-steerable reflector to illuminate the photodiode for channel 2 at the intensity expected in service and adjust the channel two gain to the desired output voltage, then steer the beam to illuminate channel 1 and take the ratio of channel outputs to compute the gain ratio. When this operation was performed, the actual gain ratio was consistent with the

TABLE 3

Internal Controls (top to bottom)

Potentiometer	Function
1	Gain Resistor Channel 2
2	Gain Resistor Channel 1
3	Offset, Stage 1 Channel 1
4	Offset, Stage 1 Channel 2
5	No Connection
6	No Connection
7	Offset, Stage 3, Channel 1
8	Offset, Stage 3, Channel 2
9	Offset, Servo Signal Filter
10	Offset, Micrometer Signal

gain ratio set on stage 1 for each channel and the tolerances of the fixed resistors used for the input and output resistors for the remaining amplifier stages. This implies that the channel response is linear with signal intensity.

The offset potentiometers for each stage in each channel can be zeroed sequentially using a good multimeter. A contact is provided on the card for connection of the multimeter low to ground, and for the output of each stage. Note that the offset for stage 2 of a given channel is an external control. Zeroing a stage by grounding the input can very easily lead to the overload of the previous stage resulting in loss of the operational amplifier. Measurement of a stage gain resistance can only be accomplished with the circuitry card removed from the socket. Setting the offset potentiometers is accomplished with the card plugged in and the power on, with the photodiodes covered.

The servo signal filter may be zeroed as follows. Short the outputs of channel 1 to channel 2 using the appropriate stings on the circuitry card and a jumper cable. Adjust the potential to ground of the filter input to zero volts using the external control. Then adjust the potential to ground of the filter output to zero volts using the offset potentiometer.

The micrometer summing amplifier may be biased as follows. Adjust potential to ground of the input pin of the summing amplifier to zero volts using the external control. Then zero the potential to ground of the output of the summing amplifier using the offset potentiometer.

3. External Controls and Connections

The device normally has four outputs for which coaxial sockets have been provide on the back mounting plate. They are, from left to right, channel 1, channel 2, the servo-signal output, and the micrometer zoom position signal. A knob which adjusts the zero for each of these outputs is located just above the appropriate jack. These zero knobs can be adjusted using the appropriate chart pen after the chart has been zeroed according to its instruction manual. The channel outputs should be zeroed with the laser on, and the fuel spray or particles of interest absent. The servo signal is most easily zeroed with the output of channel one shorted to the output of channel 2. Channels 1 and 2, and the servo signal output go to three pens on a three pen chart recorder. The micrometer position signal is connected to a pen on a two pen chart recorder. Do not short either channel to ground. This could overload one or more operational amplifiers, resulting in component damage. The micrometer zoom position signal may be zeroed at any desired micrometer setting.

The photodiode pair selector switch is located above and to the left of the output coaxial sockets. A cable at the base of the mounting plate supplies ground, +15 Volts, -15 Volts, and photodiode bias, if desired. Another cable goes from the base of the mounting plate to a cannon plug on the zoom drive assembly. This cannon plug is connected to the micrometer potentiometer. This same cannon plug is connected to the zoom drive motor. Another cable from this cannon plug leads to the motor drive control box.

The motor drive control box has two lights on it associated with zoom travel limit switches which are not currently functional because of problems previously discussed. Below these lights are three controls, from left to right. The first is a three position auto-off-manual switch. The middle knob is a rheostat which attenuates zoom motor driving potential when it is operated in the manual mode. The last three position switch is spring-loaded to the off position in the middle, and moving the switch to either side runs the zoom drive motor in either direction in manual mode. On the back side of the motor control box are two coaxial sockets with a cannon plug socket in the middle. Facing the sockets with the control knobs on top, the coaxial socket to the left should be connected to +28 Volts, and the one to the left should be connected to the servo-amplifier power output coaxial socket. The cannon plug socket is connected to the zoom drive assembly cannon plug.

The Hyband Servo Amplifier has a plate mounted on its side with three coaxial sockets. From left to right, they should be connected to the optical device servo signal output, +28 Volts, and to the zoom drive motor control box (this socket is the servo-amplifier power output.) The optical device servo signal output has to be split so that it can also go to the third pen of the three pen chart recorder.

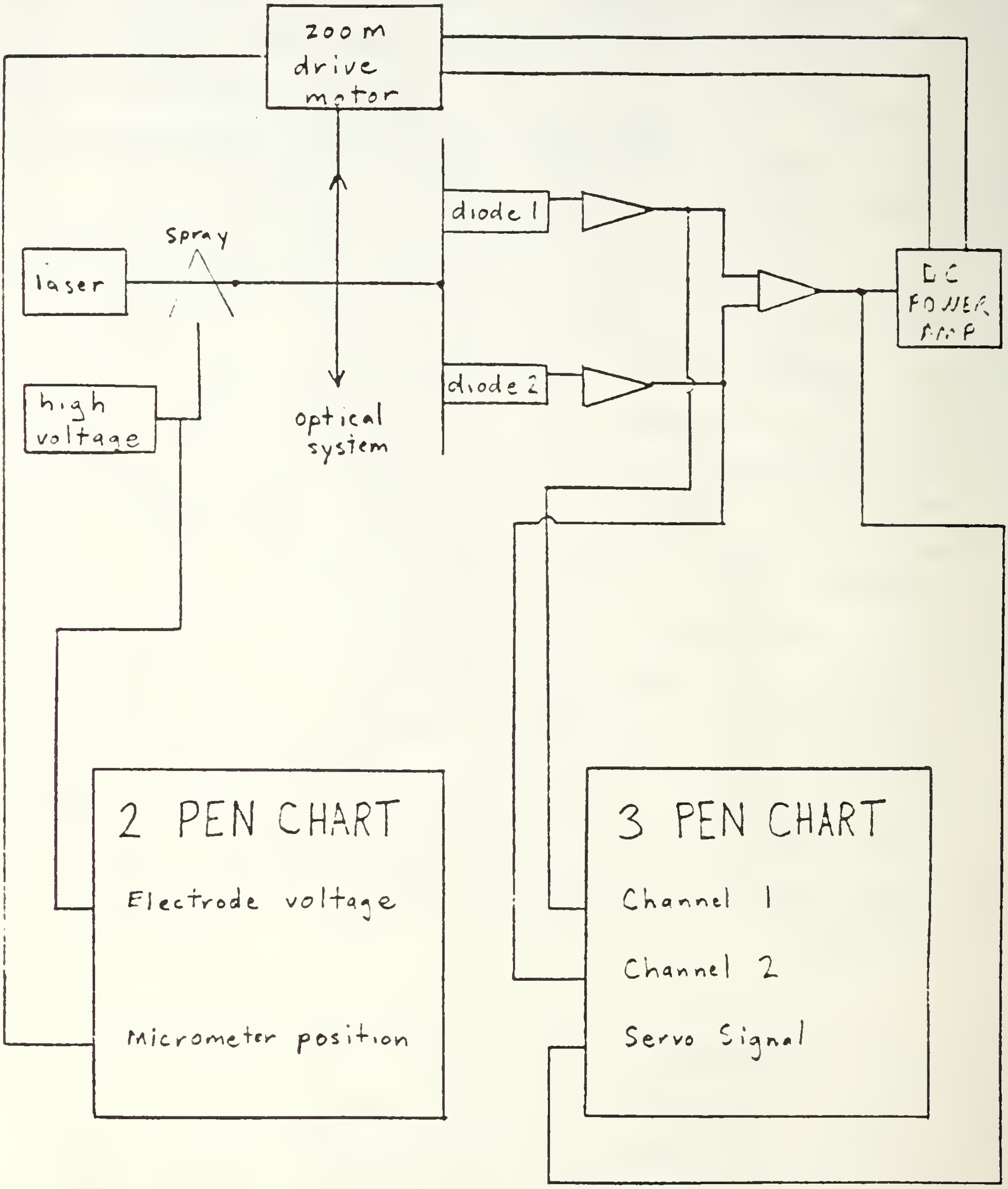

Figure 3.1 Signal Processing Block Diagram

IV. CONCLUSIONS

The droplet size of a fuel spray pattern from a T-56 nozzle using DF-2 fuel was investigated to a preliminary extent using the device described with a high intensity electric field applied and with no applied electric field. The fuel pressure was 75 psig, and a sharp electrode with the point 10 mm from the nozzle was used to apply potentials of up to 16 kV. The droplet size varied from run to run and within a run from outer limits of 42 to 48 microns, and the application of electricity had no obvious or consistent effect on the droplet size.

Figure 4.1 is a typical run of micrometric position signal versus applied voltage. The erratic trace is the micrometric position signal. The other trace is the applied voltage which starts out at 16 kV and then is decreased to zero Volts.

Figure 4.2 is the trace from the three pen recorder for the same run. The fat trace is the servo-signal output. The other trace is the superimposed traces of channels one and two. A split of channel signals of less than one percent is sufficient to achieve the width from zero of the servo-signal output on this trace, where no split represents a zero error due to servo tracking.

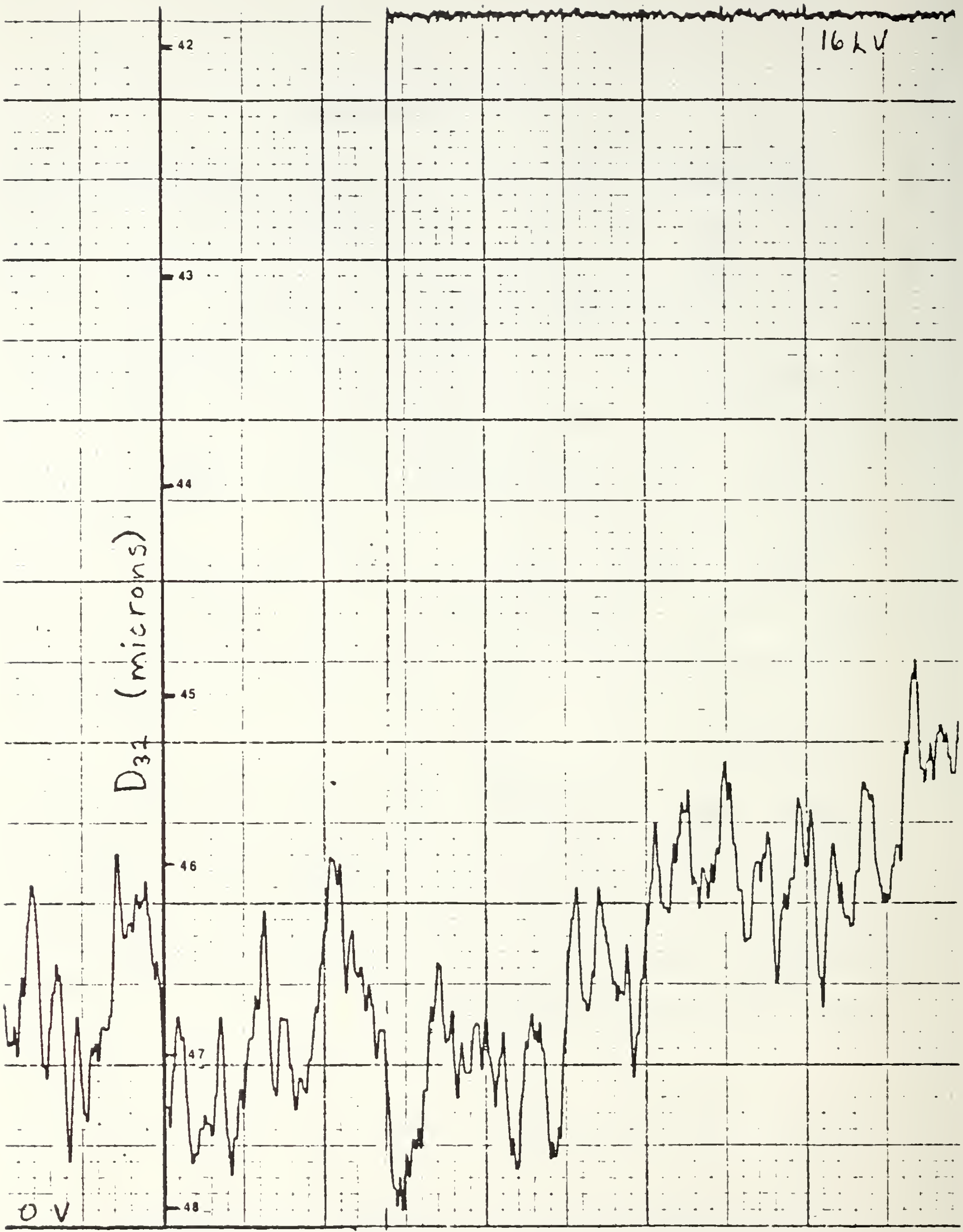

Figure 4.1 Typical D_{32} vs Electrode Voltage

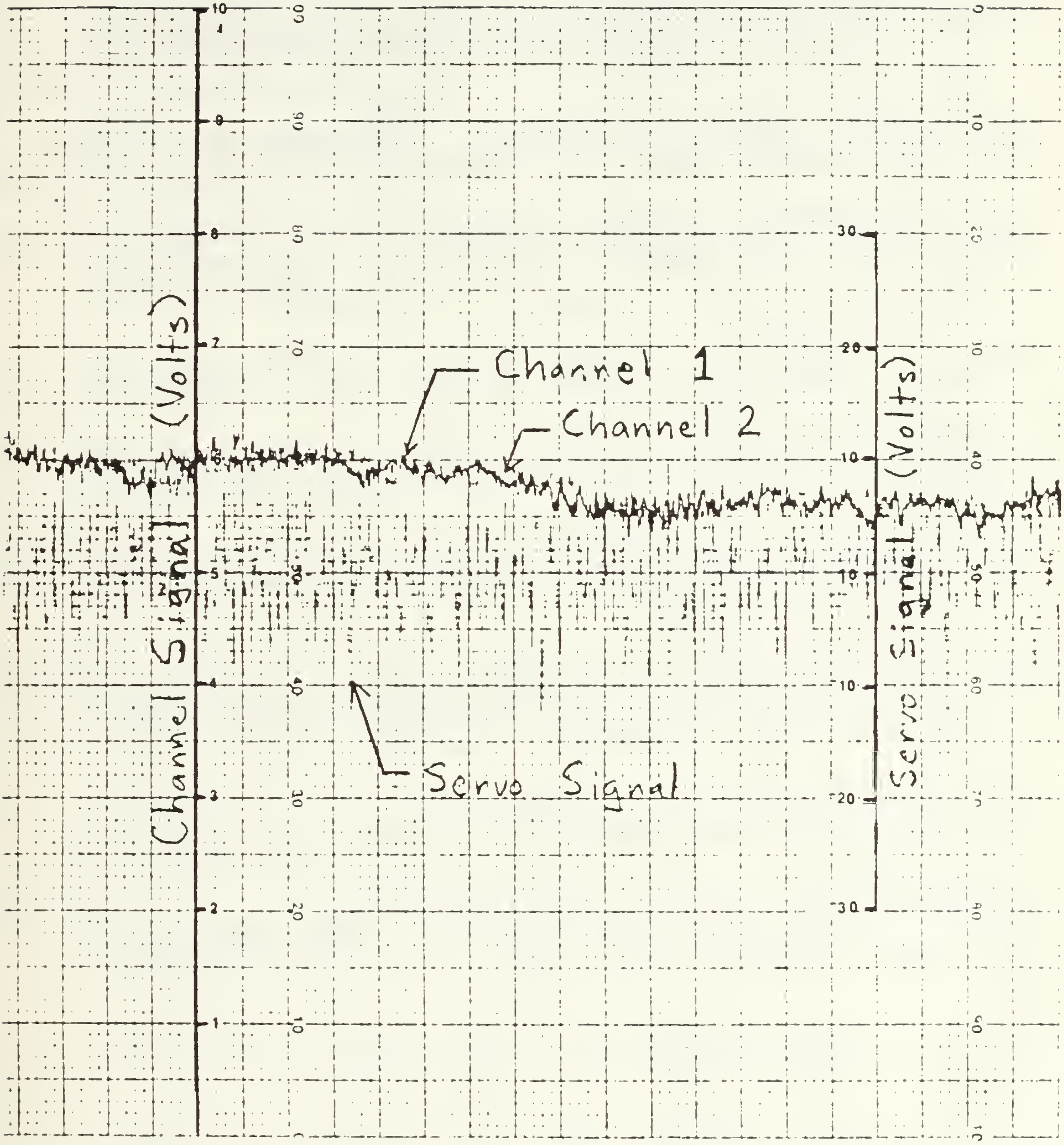

Figure 4.2   Typical Channel Response and Servo Tracking

V. RECOMMENDATIONS

The most demanding task when operating this system is obtaining and maintaining alignment of the optical system with the transmitted beam. The mounting wobbles noticeably with small applied forces at the angles of interest. At larger particle sizes at which the particle sizing device is theoretically capable of handling this unsteadiness would probably be intolerable. An isolated shock mounted optical table would make a noticeable improvement.

At present, the effective photodiode aperture is the active area of the photodiode itself. Earlier attempts at using small pinhole apertures at the aft focal point of the zoom lens resulted in a channel gain ratio that was inconsistent with the channel gain resistances by a large factor. Further work with precision made, sharp circular pinhole apertures is needed.

The device would be much easier to use if a more positive method of excluding the light through the 400 micron aperture than the present flat-black painted string, such as using a pin on a screw.

The device has the wiring in place for zoom travel limit microswitches. The switches in place are too large to be incorporated in a simple manner. Small microswitches could be used to solve the problem.

LIST OF REFERENCES

1. Mavroudis, J. A., *Experimental Study of Electrostatically Modified Fuel Sprays on Gas Turbine Combustor Performance*, M.S. Thesis, Naval Postgraduate School, Monterey, California, December 1982.

2. Laib, R. J., *Design of an Apparatus for the study of Electrohydrodynamic Control of Spray from Fuel Injectors in Gas Turbines*, A.E. Thesis, December 1982.

3. Zajdman, A., *Electrical Spray Modification with Various Fuels in a T56 Combustor*, Contractor Report, Naval Postgraduate School, Monterey, California, December 1982.

4. Van de Hulst, H. C., *Light Scattering by Small Particles*, John Wiley and Sons, Inc., 1957.

5. NASA Technical Paper 2156, *Particle Sizing by Measurement of Forward-Scattered Light at Two Angles*, by D. R. Buchelle, 1983.

6. Hodkinson, J. R., "Particle Sizing by Means of the Forward Scattered Lobe," *Applied Optics*, vol. 5, no. 5, pp. 839-844, May 1966.

7. Dobbins, R. A., Crocco, L., and Glassman, I., "Measurement of Mean Particle Sizes of Sprays from Diffractively Scattered Light," *AAIA Journal*, vol. 1, no. 8, pp. 1882-1886, August 1963.

8. Roberts, J. H. and Webb, M. J., "Measurement of Droplet Size for Wide Range Particle Distributions," *AAIA Journal*, vol. 2, no. 3, pp. 583-585, March 1964.

9. Dieck, R. H. and Roberts, R. L., "The Determination of the Sauter Mean Diameter in Fuel Nozzle Sprays," *Applied Optics*, vol. 9, no. 9, pp. 2007-2014, September 1970.

10. Hecht, E. and Zajac, A., *Optics*, Addison-Wesley Publishing Company, Inc., Chapter 5, 1979.

11. Hecht, E. and Zajac, A., *Optics*, Addison-Wesley Publishing Company, Inc., pp. 462-475, 1979.

BIBLIOGRAPHY

Boylestad, R.; and Nashelsky, L.; Electronic Devices and Circuit Theory, Prentice-Hall Inc., 1982.

Buchsbaum, W. H., Buchsbaum's Complete Handbook of Practical Electronic Reference Data, Second Edition, Prentice-Hall, Inc., 1978.

Hecht, E.; and Zajac, A.; Optics, Addison-Wesley Publishing Company, Inc., 1979.

Van de Hulst, H. C., Light Scattering by Small Particles, John Wiley and Sons, Inc., 1957.

INITIAL DISTRIBUTION LIST

		No. Copies
1.	Chairman, Code 67 Department of Aeronautics Naval Postgraduate School Monterey, Ca 93943	1
2.	Library, Code 0142 Naval Postgraduate School Monterey Ca 93943	2
3.	Professor O. Biblarz, Code 67 Bi Department of Aeronautics Naval Postgraduate School Monterey, Ca 93943	5
4.	Professor J. A. Miller, Code 67 Mo Department of Aeronautics Naval Postgraduate School Monterey, Ca 93943	5
5.	LT J. Powers VRC-30 NAS North Island San Diego, Ca 92135	2
6.	Mr. Zeev Shavit, Code 67 Department of Aeronautics Naval Postgraduate School Monterey, Ca 93943	1
7.	Commanding Officer Naval Air Systems Command Attn: Mr. G. Derderian, Code AIR 330B Washington, D.C. 20361	3
8.	Commanding Officer Naval Air Systems Command Attn: Mr. T. Momiyama, Code AIR 330 Washington, D.C. 20361	1
9.	Mr. C. D. B. Curry, ONR Patent Council Naval Station, Treasure Island Bldg 7, Room 82 San Francisco, CA 94130	2
10.	Defense Technical Information Center Cameron Station Alexandria, Virginia 23314	2

[illegible]

Thesis
P76952 Powers
c.1
Particle sizing
from forward scattered
light at two angles
using a variable-focal-
length optical system.

[illegible]

Thesis
P76952 Powers
c.1
Particle sizing
from forward scattered
light at two angles
using a variable-focal-
length optical system.

thesP76952
Partical sizing from forward scattered l
3 2768 000 61139 6
DUDLEY KNOX LIBRARY